Magnetic Properties of Tunicate Blood Cells. II. *Ascidia ceratodes*

Kenneth Kustin, William E. Robinson, Richard B. Frankel, and K. Spartalian

KK. *Department of Chemistry, Brandeis University, Waltham, Massachusetts, U.S* .—WER . *Environmental Sciences Program, University of Massachusetts–Boston, Boston, Massachusetts, U.S* .—RBF . *Department of Physics, California Polytechnic University, San Luis Obispo, California, U.S* .—KS . *Department of Physics, University of Vermont, Burlington, Vermont, U.S.*

ABSTRACT

The magnetic properties of intact blood cells of the tunicate *Ascidia ceratodes* have been measured up to 50 kOe with a SQUID susceptometer. Analysis of total metal contents by plasma emission spectroscopy and V(IV) content by epr indicates that approximately 5% of the accumulated vanadium is +4 vanadyl ion. Measured values of the magnetic moment M_P at different values of the applied magnetic field H over the temperature range $T = 2$–100 K depend on the magnitude of the field indicating magnetic anisotropy of the ground state. The slope of the M_P vs. H/T curve at high temperature is significantly higher than expected from electron spin $S = 1$ per vanadium(III) ion. The model that fits these data best is a dimer with one V(III) $S = 1$ ion ferromagnetically coupled to a second V(III) $S = 1$ ion, with spin-coupling constant $J = 3.5\ cm^{-1}$, and 5% of the total vanadium content in the form of a V(IV) $S = 1/2$ ion. Since vanadium in *A. ceratodes* is known to reside in at least three different types of blood cell, the excellent fit indicates that the metal is stored predominantly as a dimer regardless of blood cell type. Ferromagnetic coupling implies that the two vanadium ions in the dimer are connected by an unprotonated μ-oxo bridge.

ABBREVIATIONS

B. M., Bohr magneton; epr, electron paramagnetic resonance; SQUID, superconducting quantum interference device.

INTRODUCTION

Vanadium is a powerful biological effector, whether present naturally in a bromoperoxidase enzyme [1] or applied exogenously in an insulin mimetic [2]. Unlike many other essential metals, such as calcium or copper, the biological effects of vanadium are varied and depend strongly on the oxidation state [3]. One of the most puzzling naturally occurring vanadium oxidation states is V(III) in tunicate blood cells. Neither the form of this oxidation state nor the function of the accumulated metal is known with precision for any species of tunicate [4].

Three blood cell types contain virtually all of the accumulated vanadium [4]. Two such cells are colorless and contain one (signet ring cell) or at most five (compartment cell) vacuoles, in which the vanadium is thought to be stored. Another cell type containing vanadium is the yellow morula cell, which contains on average 14 vacuoles. The yellow color is due to the tunichromes, a family of powerfully reducing and chelating hydroquinoid peptides [5]. In all species where it occurs, tunichrome has been detected only in morula cells, but this finding may be misleading since the tunichrome assay only detects free (non-complexed) tunichrome. Although tunichrome may participate in the process of accumulating vanadium from seawater, where the element is in the form of vanadate(V) anion, there is evidence that the accumulated reduced vanadium and tunichrome do not interact during accumulation and storage [4, 6, 7].

In the large black solitary tunicate *Ascidia nigra* collected from Floridian ocean waters, on average, 90% of the vanadium is V(III) and 10% is V(IV) [8]. It was determined by flow cytometry that for *A. nigra*, approximately 90% of total vanadium is located in the signet ring cell [9]. In a previous paper [10], the magnetic properties of intact and freeze-dried blood cells of *A. nigra* were measured up to 50 kOe with a superconducting quantum interference device (SQUID) susceptometer along with model vanadium(III) and (IV) compounds. This study established the validity of the SQUID methodology in measuring tunicate blood cell magnetic properties, the results reconfirming the 90% V(III) and 10% V(IV) distribution found in earlier experiments.

A more widely studied tunicate species is *A. ceratodes*, a somewhat smaller, solitary, light yellow tunicate collected from Californian ocean waters. This species also synthesizes tunichrome [11], whose free form likewise has been found only in morula cells. The distribution of vanadium among *A. ceratodes* blood cell types is not identical to that of *A. nigra*, however. In *A. ceratodes*, approximately 75% of the stored vanadium is located in signet ring and compartment blood cell types; the remainder is located in morula cells [9]. The predominant oxidation state, measured by X-ray absorption [6], is vanadium(III) (90–95%, depending on seasonal and geographic factors).

In this paper, we present the magnetic properties of intact *A. ceratodes* blood cells measured for different values of the applied magnetic field over the temperature range 2–100 K.

EXPERIMENTAL

Thirty specimens of *A. ceratodes* (gathered off Monterey, CA, by Sea Life Supply and shipped the same day to our laboratories) were dissected under an

Ar atmosphere in a glove bag. The animals were very ripe, and care was taken to avoid inclusion of gonads in the blood sample. We dissected the tunic, exposing the body cavity, and pipetted the blood, which had pooled there, into a centrifuge tube. The sample was covered, removed from the glove bag, spun down, and returned to the glove bag where the supernatant was discarded and the blood pellet was loaded into a preweighed SQUID sample holder.

Magnetic moment measurements at applied fields between 5 and 50 kOe were carried out with an S. H. E. VTS-905 SQUID magnetometer operating between 2 and 100 K. Concentrations of V, Fe, and Mn were subsequently measured in each sample using a Spectrametrics Spectrospan IIIB DC plasma emission spectrometer after cold digestion with concentrated nitric acid (blood sample: 73.10 mg wet weight; V, 2.93 ± 0.08; Fe, ~ 0.06; Mn, ~ 0.006 μg/mg). Analysis of additional samples by epr spectrometry indicated that 5% of the accumulated vanadium was present as V(IV) vanadyl ion.

DATA TREATMENT AND RESULTS

The magnetic moment per molecule M_P in B.M. for *A. ceratodes* blood cells is plotted as a function of H/T in Figure 1, where H is the applied magnetic field intensity (kOe) and T is the temperature (K). The experimental data were corrected for diamagnetism following the procedure outlined in our previous paper [10]. As in the case of *A. nigra*, the value of M_P depends on the magnitude of H indicating magnetic anisotropy of the ground state. However, unlike *A. nigra*, the slope of the M_P vs. H/T curve, which, at high temperature, is proportional to $S(S+1)$, is significantly higher than expected from an assignment of $S = 1$. An assignment of $S = 3/2$ is inconsistent with previous epr results [12], which show that no more than approximately 10% of the vanadium is ever epr active, indicating that the bulk of the vanadium is in an integral spin state. This process of elimination forced us to consider spin coupling between neighboring vanadium ions as an alternative. The only coupling scheme that provides integral spin states as well as ground state anisotropy is a V(III) $S = 1$

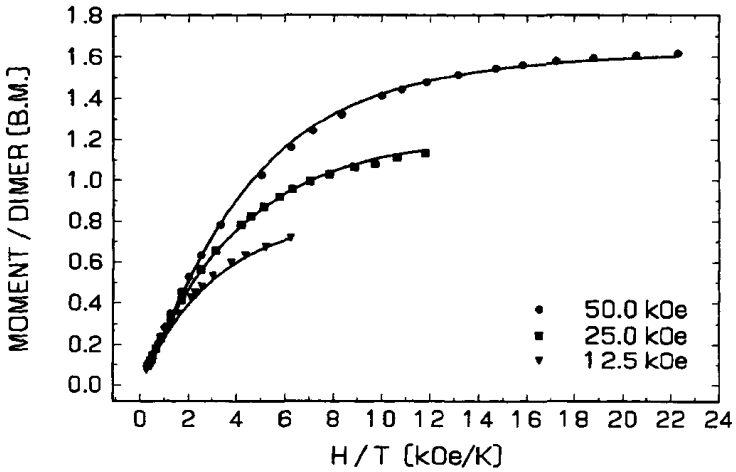

FIGURE 1. Magnetic moment per dimer vs. H/T of *A. ceratodes* whole blood cells. The solid lines are calculations at each magnetic field strength using the crystal field model as explained in the text.

ion spin-coupled to another V(III) $S = 1$ ion. Anisotropy is introduced by localized spin-orbit coupling within each ion.

For the ith ion, we write the localized, single-ion Hamiltonian in zero applied field as

$$\mathscr{H}_i = \mathscr{H}_{cf,i} + \mathscr{H}_{SO,i}, \qquad i = 1 \text{ or } 2, \tag{1}$$

where $\mathscr{H}_{cf}$ is the crystal field Hamiltonian and $\mathscr{H}_{SO}$ is the spin-orbit coupling Hamiltonian. In order to limit the size of the problem, the single-ion many-electron basis states that we used were the crystal field eigenstates described by the two-electron spin triplets $(xy)^1(zx)^1$, $(xy)^1(yz)^1$, and $(zx)^1(yz)^1$ expressed as Slater determinants. Although the size of the single-ion matrices is a manageable 9×9, the size of the spin-coupled matrices is 81×81. The crystal field matrix $\mathbf{H}_{cf}$ is diagonal in this representation. The relevant parameters are V_a and V_b, the two energy separations between adjacent spin triplets. For simplicity, we have assumed that the two spin-coupled vanadium ions have identical crystal field parameters V_a and V_b. The spin-orbit coupling Hamiltonian for the ith ion is $\mathscr{H}_{SO} = \zeta \mathbf{L}_i \cdot \mathbf{S}_i$, with $\zeta = 209\ \text{cm}^{-1}$ for V(III) [13].

The complete Hamiltonian in zero field is

$$\mathscr{H} = \mathscr{H}_1 + \mathscr{H}_2 - 2J(S_1 \cdot S_2) \tag{2}$$

where J is the spin-coupling constant. The complete Hamiltonian is represented by a matrix with dimensionality 81×81 and basis states that are the products of the single-ion states. Strictly speaking, the Zeeman interaction of the electronic magnetic moment with the applied field must be added to the matrix before diagonalization, but this step would make the fitting procedure prohibitively time consuming and complex. Instead, we treated the Zeeman interaction as a perturbation on the zero field eigenstates, and diagonalized a truncated matrix that excluded all states that are thermally inaccessible at our experimental temperatures. The dimensionality of the matrix was thus reduced to 27×27. The experimental results were fitted to the model using the method of least squares in conjunction with a simplex algorithm. There were three adjustable parameters: the crystal field splittings V_a and V_b and the spin-coupling constant J. We used the following step-by-step procedure to obtain the best parameters.

First, we diagonalized the zero field Hamiltonian (1) and obtained the 81 eigenvalues and eigenstates. These were then ordered in ascending order of energy, and the reordered unitary eigenvector matrix U was used in the unitary transformation $\mathbf{U}^\dagger\mathbf{M}\mathbf{U}$ to find the magnetic moment matrix $\mathbf{M}'$ in the diagonal representation. Matrix $\mathbf{M} = \beta(\mathbf{L} + 2\mathbf{S})$ represents the electronic magnetic moment consisting of the orbital and spin contributions; β is the Bohr magneton. The next step was to use the top left 27×27 corner of $\mathbf{M}'$ in order to calculate the Zeeman Hamiltonian

$$\mathscr{H}_{\text{Zeeman}} = \mathbf{H} \cdot \mathbf{M}' = \mathrm{H_x M'_x} + \mathrm{H_y M'_y} + \mathrm{H_z M'_z}. \tag{3}$$

For a given orientation of the applied field with respect to the crystalline xyz-axis system, the Zeeman Hamiltonian is diagonalized and the projection of the spin along the applied field is calculated. A polycrystalline average is

TABLE 1. Fitted Parameters

$V_a = -294\ cm^{-1}$
$V_b = +384\ cm^{-1}$
$J = 3.5\ cm^{-1}$

obtained by stepping the applied field direction in equal increments of solid angle over an octant of the unit sphere. In the present case, a 7×7 grid was used. In order to account for the epr active vanadium, the contribution of 5% calculated paramagnetic impurity of V(IV) as determined in this study was added as a final step.

Table 1 shows the best parameters of the fits represented as solid lines in Figure 1. Considering that this is a fit with only three adjustable parameters, it is clear that the model accounts for the data rather well. We could perhaps improve the fit by introducing additional parameters, such as separate sets of crystal field parameters V_a and V_b, as would be required by nonequivalent vanadium sites. Although such improvements may bring the calculation closer to experiment, they are not likely to change the basic features of our model: 1) vanadium in *A. ceratodes* is predominantly in the V(III) state, 2) vanadium ions are spin-coupled in pairs with positive spin-coupling constant J (ferromagnetic coupling), and 3) the observed epr signal is due to a small amount of V(IV).

We considered the use of a spin Hamiltonian treatment with spin coupling between two $S = 1$ ions, but soon abandoned this approach because it quickly became apparent that there was no unique set of parameters able to account for both the slope at high temperature and the anisotropy at low temperature. Furthermore, a spin Hamiltonian treatment of two spin-coupled $S = 1$ ions can only give a total of nine states that may or may not be all that is thermally accessible. It is perhaps instructive to examine the energy level structure of the first 27 eigenstates of the zero field Hamiltonian (1) shown in Figure 2. We see a cluster of nine singlet states with an overall width of about 60 cm^{-1}, a gap of about 250 cm^{-1}, and a second cluster consisting of 18 states which appear to be doubly degenerate in zero field. These features can be understood in terms of our model and its parameters. Each of the two ions consists of three spin triplets well separated in energy. The ground state triplet of ion 1 spin-couples with the ground state triplet of ion 2 and results in a low-lying cluster of nine states. The cluster of states lying next in energy results from the ground state triplet of ion 1

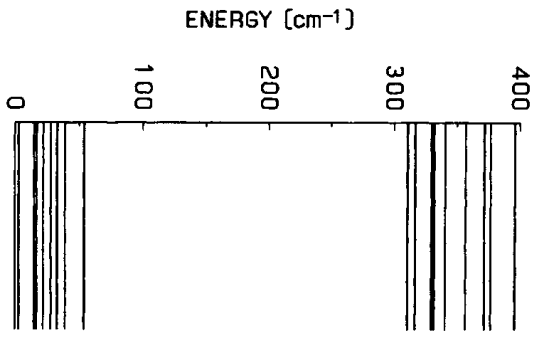

FIGURE 2. Energy level diagram of the first 27 eigenstates of the zero field Hamiltonian [Equation (2)]. Because of the accidental degeneracy of the upper multiplet, only 18 states are shown.

spin-coupling with the first excited state triplet of ion 2, and from the first excited state triplet of ion 1 spin-coupling with the ground state triplet of ion 2. This spin coupling produces a total of 18 states which will be degenerate in pairs if, as we have assumed here, ions 1 and 2 are indistinguishable by having identical triplet structures. Thus, the degeneracy is accidental and an artifact of our model.

DISCUSSION

The strong predominance of a vanadium(III) dimer signifies that the accumulation of this element in *A. ceratodes* is different from that of *A. nigra* where no evidence of dimer was found. It is generally agreed that the blood of *A. ceratodes* contains at least two [9], and very likely three [14], different types of vanadium-containing blood cells. Since significant quantities of vanadium are present in at least three blood cell types, according to this model, the vanadium structure and environment must be reasonably uniform in the different vanadium-accumulating blood cells. Although coordination to accumulated vanadium appears to involve only oxygen atoms [6], persistence of the same type of dimeric structure in each blood cell type is not *a priori* expected; nevertheless, we find evidence for only one structure.

While considering vanadyl epr as a probe of pH in ascidian blood cells, Frank et al. [12] calculated that 28% of the accumulated vanadium might be dimeric, but rejected this conclusion because no effect of V(III) dimers on the X-ray absorption data were observed. However, in a study based on assignment of an absorbance shoulder at 415 nm in the optical spectrum of *A. ceratodes* blood cells, Anderson and Swinehart [14] concluded that about 15% of the total accumulated vanadium was in the form of a dimer. Addition of the chelating agents 2,2′-bipyridine and 1,10-phenanthroline to various Aplousobranch and Phlebobranch ascidians resulted in the formation of a purple–black complex in compartment and signet ring cells. Extraction and examination of this complex led Brand et al. [7] to the conclusion that this complex was a divanadium oxo-bridged dimer. Our studies provide the first direct determination of the predominance of a vanadium(III) dimer in *A. ceratodes*. This model indicates that virtually all of the vanadium(III) is present in dimerized form. Because the dimer is essentially absent in *A. nigra*, we conclude that either this form of accumulated vanadium is only present in a few species of tunicates, or that geographic and seasonal differences could influence the prevalence of dimerization.

A further insight into the nature of the environment of the vanadium dimer can be obtained by comparison with model compounds. Studies of the magnetic properties of divanadium oxo-bridged complexes reveal either strongly coupled (ferromagnetic or antiferromagnetic), weakly coupled, or noncoupled vanadium ions [15], depending on ligand, solvent, pH, and other conditions. Upon being protonated, complexes with ferromagnetic coupling change to antiferromagnetic coupling [16, 17]. Carrano et al. [17] crystallized both protonated and deprotonated divanadium compounds for a particular ligand, and located structural changes as a consequence of protonating the oxo-bridge that accounts for the change from ferromagnetic coupling to antiferromagnetic coupling. The native vanadium(III) dimer in *A. ceratodes* is weakly ferromagnetically coupled, consis-

tent with *ab initio* calculations of magnetic exchange coupling in linear oxo-bridged binuclear complexes of V(III) [18]. Since antiferromagnetic coupling is associated with protonation, our results imply that intracellular conditions in the vicinity of the native vanadium(III) dimer are not sufficiently acidic to protonate the oxo-bridge.

This research was supported in part by Research Grant DCB-8500309 from the National Science Foundation and in part by Research Grant GC-R-32189-7 from the MIT / SeaGrant. Additional support for R. B. F. from the National Science Foundation is also acknowledged. We thank Prof. N. Dennis Chasteen and Dr. Phillip Hanna for providing the epr analysis of our sample, and Prof. C. Carrano for stimulating and helpful discussions.

REFERENCES

1. R. Wever and K. Kustin, *Adv. Inorg. Chem.* **35**, 103 (1990).
2. N. D. Chasteen, *Vanadium in Biological Systems*, Kluwer Academic Publishers, Dordrecht, 1990, pp. 1–225.
3. D. W. Boyd and K. Kustin, *Advances in Inorganic Biochemistry, Vol. 6*, G. L. Eichhorn and L. G. Marzilli, Eds., Elsevier, New York, 1984, pp. 311–365.
4. R. Martoja, P. Gouzerh, and F. Monniot, *Oceanography and Marine Biology: An Annual Review* **32**, 531 (1994).
5. M. J. Smith, D. Kim, B. Horenstein, K. Nakanishi, and K. Kustin, *Acc. Chem. Res.* **24**, 117 (1991).
6. T. D. Tullius, W. O. Gillum, R. M. K. Carlson, and K. O. Hodgson, *J. Amer. Chem. Soc.* **102**, 5670 (1980).
7. S. G. Brand, C. J. Hawkins, A. T. Marshall, G. W. Nette, and D. L. Parry, *Comp. Biochem. Physiol.* **93B**, 425 (1989).
8. A. L. Dingley, K. Kustin, I. G. Macara, and G. C. McLeod, *Biochim. Biophys. Acta* **649**, 493 (1981).
9. E. M. Oltz, S. Pollack, T. Delohery, M. J. Smith, M. Ojika, K. Lee, K. Kustin, and K. Nakanishi, *Experientia* **45**, 187 (1989).
10. S. Lee, K. Kustin, W. E. Robinson, R. B. Frankel, and K. Spartalian, *J. Inorg. Biochem.* **33**, 183 (1988b).
11. D. L. Parry, S. G. Brand, and K. Kustin, *Bull. Marine Sci.* **50**, 302 (1992).
12. P. Frank, R. M. K. Carlson, and K. O. Hodgson, *Inorg. Chem.* **25**, 470 (1986).
13. J. S. Griffith, *The Theory of Transition-Metal Ions*, Cambridge University Press, Cambridge, 1961, p. 437.
14. D. H. Anderson and J. H. Swinehart, *Comp. Biochem. Physiol.* **99A**, 585 (1991).
15. S. L. Castro, M. E. Cass, F. J. Hollander, and S. L. Bartley, *Inorg. Chem.* **34**, 466 (1995).
16. P. Knopp and K. Wieghardt, *Inorg. Chem.* **30**, 4061 (1991).
17. C. J. Carrano, R. Verastgue, and M. R. Bond, *Inorg. Chem.* **35**, 3589 (1993).
18. K. Fink, R. Fink, and V. Staemmler, *Inorg. Chem.* **33**, 6219 (1994).